Structures, energetics, and infrared spectra of the Cl^-–$(H_2S)_n$ and Br^-–$(H_2S)_n$ anion clusters from *ab initio* calculations†

D. A. Wild*[ab] and T. Lenzer[b]

Received 3rd July 2007, Accepted 3rd September 2007
First published as an Advance Article on the web 13th September 2007
DOI: 10.1039/b710111b

Anion clusters formed between a chloride or bromide anion and H_2S molecules have been investigated using *ab initio* methods. Cluster structures, binding energies, and vibrational properties were predicted at the MP2 level with basis sets of aug-cc-pvtz and aug-cc-pvdz quality. Vibrational self consistent field (VSCF) calculations were employed to correct the predicted harmonic vibrational frequencies of the dimer complexes for anharmonicity. The major finding of this work is that the clusters all feature "solvated anion" structural motifs, with an anion bound to perturbed, yet intact, H_2S ligands. The binding energies of the H_2S ligands to the anion decrease with larger cluster size, and this is reflected in blue shifted vibrational stretching frequencies.

1. Introduction

Intermolecular interactions play a dominant role in many contexts, from the dissolution of solutes in solution, the condensation of the noble gases, and the very structure of DNA. Furthermore the role of these interactions should not be underplayed in the transition states of reactions, and also in the reactive Van der Waals wells observed in some reaction potential energy surfaces.[1,2] In this way, loosely bound complexes and clusters have a dramatic effect on the rate and direction of chemical change.

One line of interest in the role of intermolecular interactions has been to investigate the clusters formed between ions and solvent molecules, aimed towards a better understanding of solvation in bulk contexts. Numerous studies have appeared towards this end, both experimental[3–5] and theoretical[6–9] illustrating that one can build up the number of solvent molecules around an ion and thereby follow solvation in a step wise manner. A vast majority of the work undertaken has concentrated on ion–water complexes and clusters, not surprising due to water's importance in many contexts.

We are primarily interested in systems that involve solvating partners other than water, to better understand solvation in non-aqueous media. This is highlighted in our previous publications on the fluoride–ammonia,[10] and fluoride–hydrogen sulfide clusters.[11] For the latter, we predicted structures which involved proton transfer from H_2S to a fluoride anion to form the $FH\cdots SH^-$ structure. This structural motif is predicted to dominate the cluster forms when more H_2S molecules congregate around the ion core. A "solvated fluoride" structure was only observed for clusters of $n = 3$ and larger.[11]

The current work is an extension of the fluoride–hydrogen sulfide investigation, whereby here we are concentrating on the chloride and bromide ions interacting with H_2S molecules. From the outset, one would expect that the proton transfer form observed for the fluoride clusters would not exist in the analogous chloride and bromide cases. This expectation is due to the fact that the proton affinities of the chloride and bromide anions are less than for the SH^- anion (PAs 350.8, 333.4, and 323.5 kcal mol^{-1} for SH^-, Cl^-, and Br^-, respectively; ref. 12–14). We aim to predict cluster structures, and also the vibrational properties to provide a theoretical base for future experimental studies.

The Cl^-–H_2S complex has been investigated previously. The most recent investigation by Masamura reported the interaction energy of the complex at the complete basis set (CBS) limit.[15] This was achieved by calculating the geometry at the MP2/aug-cc-pvdz level of theory and following on with larger basis set electronic energy calculations. Masumura arrived at a CBS limit binding energy of 13.8 kcal mol^{-1} at the MP2 level of theory using Dunning's augmented correlation consistent basis sets (aug-cc-pvxz, with x = d, t, q and 5). In this study, structural data were not supplied, only a schematic of the cluster structure. An earlier investigation, by Del Bene, provided structures and enthalpies of formation for the Cl^-–H_2S complex.[16] The intermolecular distance, between Cl^- and sulfur, was predicted to be 3.533 Å at the MP2/6-31G + (d,p) level of theory. This study predicted a cluster binding energy of 12 kcal mol^{-1}, in line with a result quoted in an experimental paper by Larson and McMahon.[17] However, on reviewing the literature we found that the experimental value of 12 kcal mol^{-1} quoted by Larson and McMahon was unfounded. Therefore, to the best of our knowledge, there have been no experimental studies performed on these systems, and certainly no experimental or theoretical investigations of the larger clusters.

[a] *Chemistry M313, School of Biomedical, Biomolecular and Chemical Sciences, The University of Western Australia, 35 Stirling Highway, Crawley, Western Australia, 6009, Australia. E-mail: duncan.wild@uwa.edu.au; Fax: +61 8 6488 1005; Tel: +61 8 6488 3178*
[b] *MPI für biophysikalische Chemie, Abteilung Spektroskopie und Photochemische Kinetik (10100), Am Faßberg 11, D-37077 Göttingen, Germany*

† Electronic supplementary information (ESI) available: Calculated data for Br^-–$(H_2S)_n$ and Cl^-–$(H_2S)_n$ clusters. See DOI: 10.1039/b710111b

The present article aims to redress this situation and predict the structures, energetics, and infrared spectra of the dimer and larger clusters. We aim to provide bench mark data for future experiments. The computational methodology (MP2 level with Dunning's augmented correlation consistent basis sets) was chosen as it has proven successful in treating analogous halide–water clusters.[18–20] The key issue here is that to describe the diffuse nature of the anions, a basis set with diffuse functions is required. Dunning's basis sets are used, as they are tuned for electron correlation methodologies, such as MP2.

The presented results will be ideally suited for comparison with data from gas phase ion beam spectroscopic experiments. These experiments would target solely the anion clusters, leading to vital information on the solvation of anions. Similar calculations (and indeed experiments) could be performed on cation systems.

2. Methodology

The halide–$(H_2S)_n$ clusters were investigated at the MP2 level of theory using Dunning's augmented correlation consistent polarized valence sets.[21–23] Calculations were performed with basis sets of double and triple-ζ quality (aug-cc-pvxz where x = d, t) for the smaller clusters with up to three H_2S ligands interacting with the anion. The larger clusters were investigated with the aug-cc-pvdz basis set due to smaller computation times compared with using aug-cc-pvtz basis sets. Only the valence electrons were included in the MP2 calculations (frozen core approximation). Calculations were also performed for the bare species H_2S, Cl^-, and Br^- to aid in predicting cluster intermolecular binding energies. Corrections for basis set superposition error (BSSE) in the binding energies were estimated using the method of Boys and Bernardi.[24] Harmonic vibrational frequencies were computed for all cluster sizes, and it should be noted that anharmonicity of the vibrational modes is neglected in these calculations. In order to improve the predictions of the vibrational frequencies, vibrational self consistent field calculations (VSCF) were performed for the 1 : 1 dimer complexes, using the method implemented in GAMESS.[25,26] The correlation consistent variant of this method was also implemented (CC-VSCF). Natural bond order (NBO) analyses were performed on the clusters to determine the nature of the interaction between the cluster constituents.[27] Enthalpy changes for the ligand association reactions at 298 K were estimated using the method of Del Bene *et al.* described in ref. 28. The enthalpy values are equivalent to the binding energy of the H_2S ligand to the anion core for the n = 1 clusters, and indeed to the subsequent binding energy of each additional H_2S ligand in the larger clusters X^-–$(H_2S)_n$. The two terms "ligand association enthalpy" and "ligand binding energy" are used interchangeably throughout this paper.

The geometry optimisations, energy and vibrational frequency calculations, and NBO analyses were performed with the GAUSSIAN-03 program suite.[29] Diagrams of the cluster structures were produced using the gOpenMol program.[30,31]

3. Results and discussion

A. The Cl^-–H_2S and Br^-–H_2S dimer complexes

I. Structures and energetics. The 1 : 1 dimer complexes were investigated at the MP2 level of theory, using the aug-cc-pvdz and aug-cc-pvtz basis sets. Three stationary points were located for both chloride– and bromide–H_2S complexes (Fig. 1). Complete data sets including structural parameters and predicted vibrational frequencies can be found in the ESI.† We found that the use of the larger basis set (aug-cc-pvtz) did not drastically change the structural or vibrational parameters, indicating that for our subsequent studies on the larger clusters the aug-cc-pvdz basis set should suffice in describing the cluster properites (*vide infra*).

For both halides we found one minimum, of C_s symmetry, and two transition states each with C_{2v} symmetry (each with one imaginary frequency). The C_s symmetry minimum features a single H-bond between the anion and a perturbed, yet intact, H_2S molecule. As will be discussed shortly, this is in stark contrast to the analogous F^-–H_2S complex.

The intermolecular interaction between anion and ligand is confirmed to be hydrogen bonding (H-bonding) from NBO analysis. For both chloride and bromide complexes there is significant electron density transfer from the halide anion lone pair orbitals to the σ^* antibonding orbital of the H–S involved in the H-bond. In total there is 101 and 82 me of electron density transfer in the Cl^-–H_2S and Br^-–H_2S complexes, respectively. The smaller extent of charge delocalisation for the bromide complex is reflected in the H-bond length which increases from 1.990 Å for Cl^-–H_2S to 2.207 Å for Br^-–H_2S (MP2/aug-cc-pvtz results). We predict a $Cl^-\cdots S$ distance of 3.397 Å at the MP2/aug-cc-pvtz level of theory. This is

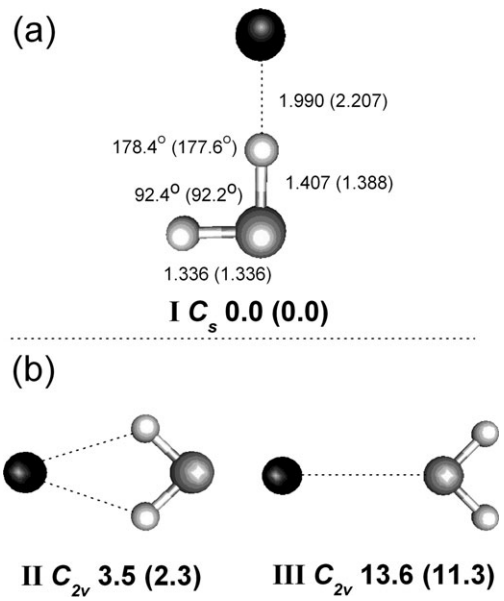

Fig. 1 Predicted stationary points of the Cl^-–H_2S and Br^-–H_2S complexes, where (a) is a minimum and (b) are higher order points (each with 1 imaginary frequency). Bond lengths and angles are provided for the minimum, with the numbers below the points corresponding to BSSE and zpe corrected energy differences. Values for the bromide complex are given in parentheses.

somewhat shorter than the previously determined value, by Del Bene, of 3.533 Å. This discrepancy is to be expected, as increasing the basis set size by the addition of more diffuse functions generally leads to contracted intermolecular bond lengths. The S–H bond distance to the hydrogen involved in H-bonding also reflects a weaker H-bond for the Br^-–H_2S complex, with $r(S–H_b) = 1.407$ and 1.388 Å for Cl^-–H_2S and Br^-–H_2S, respectively. The S–H bond to the terminal hydrogen is predicted to be the same for both complexes, at $r(S–H_t) = 1.336$ Å.

The difference in predicted enthalpy changes for the ion-ligand association reaction is consistent with the structural results. The values of $\Delta H_{0\rightarrow 1}^{298K}$ are −13.6 and −11.1 kcal mol^{-1} for the Cl^-–H_2S and Br^-–H_2S complexes, respectively. The value of 13.6 kcal mol^{-1} is somewhat higher than the value determined by Del Bene (12 kcal mol^{-1}), however as no experimental result is available it is not possible to comment on the reliability of our result compared to Del Bene's.

As stated previously, the form of both the Cl^-–H_2S and Br^-–H_2S complexes was expected to be quite different to that of the previously reported F^-–H_2S 1 : 1 complex. This expectation was confirmed, as the chloride and bromide–H_2S complexes feature a perturbed yet intact H_2S ligand, as opposed to the proton transfer structure predicted for fluoride–H_2S. One can reconcile the difference by noting that the proton affinity of the fluoride anion exceeds that of SH^-, and therefore the intermediate proton transfers from the H_2S to the F^-, forming the $FH\cdots SH^-$ structure.[11] As the proton affinities of Cl^- and Br^- are both less than that of SH^- it is not surprising that the complexes have the 'solvated' halide form shown in Fig. 1a (PAs 350.8, 333.4, and 323.5 kcal mol^{-1} for SH^-, Cl^-, and Br^-, respectively; ref. 12–14). An attempt was made to isolate proton transfer forms for the chloride and bromide complexes, however the end result of these geometry optimisations was always the structure featured in Fig. 1a. In these trials, no restrictions were placed upon the geometry, in terms of freezing coordinates.

The two Cl^-–H_2S transition states shown in Fig. 1b lie 3.5 and 13.6 kcal mol^{-1} to higher energy from the C_s minimum (2.3 and 11.3 kcal mol^{-1} for the bromide complex). The imaginary frequency for each complex is of b_2 symmetry and corresponds to a concerted bending and stretching of the H_2S towards the minimum structure. The structure labelled II in Fig. 1b features a double H-bond between H_2S and the halide, whereas for the second structure (III) the halide is interacting with the sulfur of the H_2S ligand. The double hydrogen bond is confirmed by NBO analyses where there is approximately 7 me of electron density transferred to both H-bonded S–H groups for the chloride and bromide complexes.

II. Predicted harmonic and CC-VSCF infrared spectra. Vibrational stick spectra for the Cl^-–H_2S and Br^-–H_2S complexes predicted from MP2/aug-cc-pvtz calculations are provided in Fig. 2. The lowest wavenumber vibrations correspond to the intermolecular stretching and two bending vibrations (in plane and out of plane bending). The band predicted at around 1200 cm^{-1} corresponds to the HSH intramolecular bending mode. The most intense band in each spectrum arises from motion of the H-bonded hydrogen, and appears at 1941 and 2157 cm^{-1} for Cl^-–H_2S and Br^-–H_2S, respectively. The free S–H stretching mode is predicted to lie to higher wavenumber, however is of very low intensity (<5 km mol^{-1}).

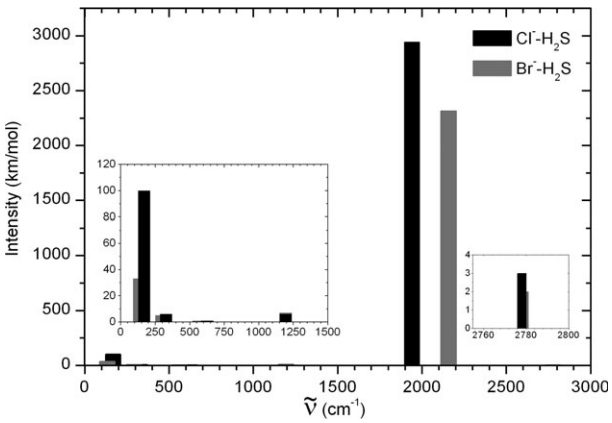

Fig. 2 Predicted harmonic infrared stick spectra of Cl^-–H_2S and Br^-–H_2S at the MP2/aug-cc-pvtz level.

For both complexes, the H-bonded S–H stretch has shifted to lower wavenumber with respect to the centroid of the predicted position of the symmetric and antisymmetric S–H stretching modes of bare H_2S, $\omega = 2783$ cm^{-1} (refer to the ESI for calculate H_2S data†). The predicted band shifts are $\Delta\omega = 842$ and 626 cm^{-1} for Cl^-–H_2S and Br^-–H_2S, respectively. The larger shift predicted for the chloride complex, reflects the increased intermolecular H-bond strength and subsequent larger perturbation on the bonded S–H group.

A comparison of the pure harmonic spectra and predictions based on CC-VSCF theory are shown in Fig. 3 for the chloride–H_2S complex. Both spectra are produced at the MP2/aug-cc-pvtz level of theory. The largest effect is observed for the H-bonded S–H stretching mode, where the band has shifted some −552 cm^{-1} to lower wavenumber, to 1389 cm^{-1}. The shift for the free S–H stretch is smaller at around −100 cm^{-1}. For the bromide complex, the H-bonded S–H stretching band has shifted −264 cm^{-1} to lower wavenumber, giving an estimated position of 1893 cm^{-1}. CC-VSCF studies of similar anion–ligand complexes have produced bands that

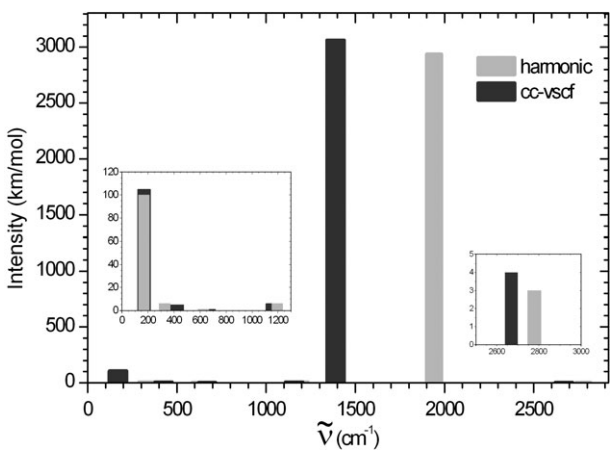

Fig. 3 Comparison between predicted harmonic and CC-VSCF infrared stick spectra of the Cl^-–H_2S complex at the MP2/aug-cc-pvtz level.

are in quite good agreement with experimental studies,[32] so we are confident that the quoted band position should be accurate to within 50 cm^{-1}.

A modification to the VSCF method has been made, whereby a quartic force field is used to produce the VSCF potential energy surfaces (VSCF-QFF).[33] In essence a reduced number of potential energy points is computed, and these points are extrapolated thereby producing 16 points for diagonal potentials, and 16 × 16 grid for mode coupling. We tested this method against the normal VSCF procedure, and found that apart from the stretch of the H-bonded hydrogen in the Cl^-–H_2S complex the computed vibrational frequencies differed by no more than 30 cm^{-1}. The larger deviation for the Cl^-–H_2S complex was observed for both levels of theory tested. The question then is, why would this mode alone show larger deviations? We can speculate that the deviation is due to the increased binding energy of the chloride complex, with respect to the bromide complex. The increased interaction leads to a greater delocalisation of the shared proton between the Cl^- and SH^- bases, and enhanced anharmonicity of the S–H stretching mode. Therefore the QFF approximation, with fewer calculated points, does rather poorly in defining the potential energy surface for this stretching mode, compared with the more complete standard VSCF method.

A second method we have implemented to compute the stretching vibrational frequencies of the *ab initio* determined cluster structures is to model the stretching modes with simplified one dimension potential energy curves. To this end we performed potential energy scans at the MP2/aug-cc-pvtz level of the H-bonded S–H stretching motion for both the chloride and bromide complexes (Δr = 0.01 Å, $r(S–H_b) \cong 0.4 \rightarrow 3.4$), with the remainder of the complex frozen (bond lengths and angles). The LEVEL 7.5 program was then used to solve the one dimensional Schrödinger equation for a pseudo diatomic thereby producing the H-bonded S–H stretching frequencies.[34]

An example of the resulting potential energy curve for the chloride–H_2S complex can be seen in Fig. 4, as a function of the S–H stretching coordinate. The first five S–H stretching levels are included on the plot, with the associated wavefunctions (both calculated using LEVEL 7.5). This simple approach produced H-bonded S–H stretching frequencies of 1438 and 1847 cm^{-1} for chloride and bromide complexes, respectively. We tested the effect of describing the reduced mass of the stretching mode in terms of purely S–H, or in terms of a S(H)–H with the mass of SH collapsed onto a single particle. The differences in the resulting vibrational frequencies for the $1 \leftarrow 0$ transition were around 1–2 cm^{-1}.

The LEVEL 7.5 results compare well with values of 1425 and 1859 cm^{-1} computed using the VSCF method (not CC-VSCF) which uses pure diagonal potentials computed from the vibrational modes neglecting mode coupling. The favourable comparison can be rationalised by the fact that the two techniques are similar methodologies.

Comparing the calculated one dimensional potential energy curves for the H-bonded stretch of the chloride and bromide–H_2S complexes, one can visualise the increased anharmonicity of the H-bonded S–H stretching mode for the former in Fig. 5. The chloride–H_2S stretching potential is markedly flatter, indicative of increased delocalisation of the shared proton compared with the bromide–H_2S complex. This comparison adds weight to our explanation of the shortcomings of the QFF approximation to the VSCF procedure for the chloride–H_2S complex, as a reduced number of points would not accurately reproduce the potential following extrapolation.

Finally, the predicted binding energies of the chloride and bromide dimer complexes are 4757 and 3882 cm^{-1}, indicating that vibrational predissociation is not a feasible method to study these complexes. This is due to the fact that excitation of the H-bonded S–H stretching vibrations does not provide the complex with sufficient energy to dissociate. Using argon tagging will certainly address this problem,[35–38] as the binding energy of argon to chloride and bromide anions is much less than the S–H stretching frequency (binding energies of X^-–Ar = 494 and 418 cm^{-1} for Cl^- and Br^-, respectively[39,40]).

B. Trimer clusters: Cl^-–$(H_2S)_2$ and Br^-–$(H_2S)_2$

I. Structures and energetics. The trimer clusters, X^-–$(H_2S)_2$, were investigated with both aug-cc-pvdz and

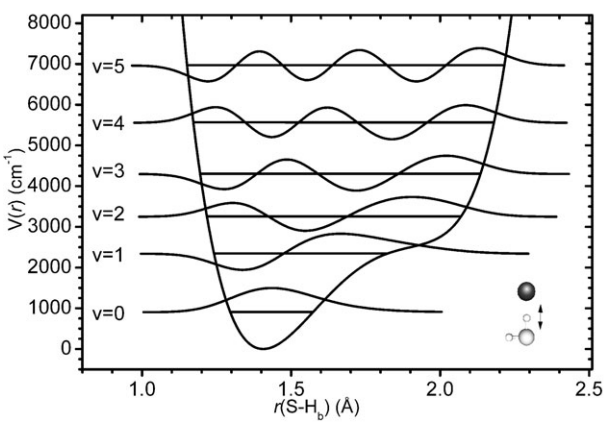

Fig. 4 One dimensional potential energy curve describing the H-bond S–H stretching mode. The supported vibrational energy levels and wavefunctions were calculated using the LEVEL 7.5 program.

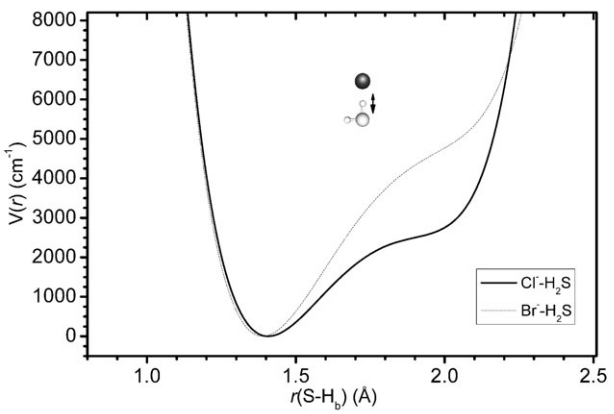

Fig. 5 Comparison of the Cl^-–H_2S and Br^-–H_2S one dimensional potential energy curves used to predict the H-bonded stretching frequency from the LEVEL 7.5 program.

aug-cc-pvtz basis sets at the MP2 level of theory. For both Cl^- and Br^-–$(H_2S)_2$ clusters we located four stationary points, however for each halide only one of the four points is predicted to be a minimum on the potential energy surface. The minimum energy structure is shown in Fig. 6a, while the higher order stationary points are shown in Fig. 6b. A full list of structural parameters can be found in the ESI.†

The minimum energy structure is of C_1 symmetry, and features an H-bond between the two H_2S ligands. This interaction was confirmed to be H-bonding by a NBO analysis which predicted significant electron density transfer between the sulfur lone pair orbitals and the σ* orbital of the bonding S–H group. The ligand association enthalpies of the chloride and bromide–$(H_2S)_2$ trimer clusters are estimated to be −10.5 and −9.4 kcal mol^{-1} at the MP2/aug-cc-pvtz level, with respect to the dimer complexes.

It should be noted that there are some differences in structural parameters on increasing the basis set size from aug-cc-pvdz to aug-cc-pvtz, most noticeably in the $HSH\cdots SH_2$ H-bond angle, and in the halide-H_2S H-bond length. However, we find that the predicted ligand binding energies and vibrational frequencies are similar (see ESI†). We therefore feel that it is justified to use the aug-cc-pvdz basis set for the larger clusters (*vide infra*).

The structures of the chloride and bromide–H_2S trimer clusters are quite different to the previously studied F^-–$(H_2S)_2$ cluster. For the latter the form was of a solvated $(FH\cdots SH)^-$ core. This is again attributed to the larger proton affinity of the fluoride anion compared with the chloride and bromide anions, which serves to abstract a proton from one of the H_2S ligands. In comparison, the chloride and bromide–$(H_2S)_n$ clusters feature a "solvated anion" structural motif.

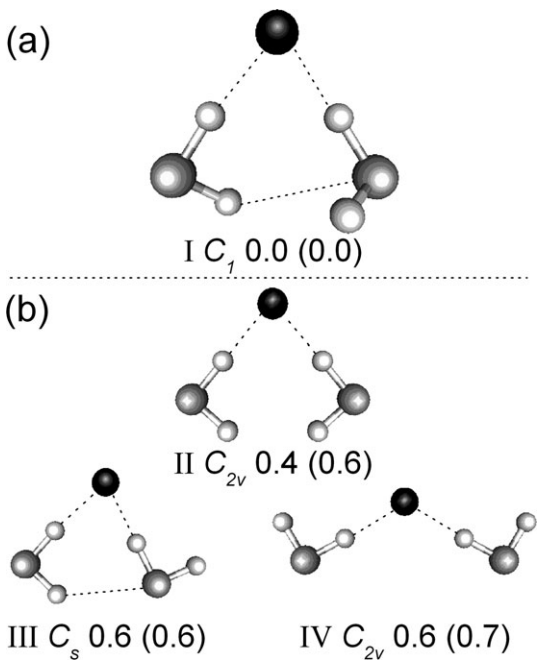

Fig. 6 Predicted stationary points of both Cl^- and Br^-–$(H_2S)_2$ trimer clusters, with (a) being a minimum, and (b) higher order stationary points (II and III with one imaginary frequency, IV with two). Numbers correspond to BSSE and zpe corrected energy differences in kcal mol^{-1} (numbers in parentheses are for Br^-–$(H_2S)_2$).

II. Predicted infrared spectra. Predicted vibrational frequencies and IR intensities are provided in the ESI for all four Cl^- and Br^-–$(H_2S)_2$ stationary points. Stick spectra of the chloride and bromide trimer minima are shown in Fig. 7. The most noticeable difference between the chloride and bromide spectra is that the H-bonded S–H stretching modes appear at higher wavenumbers for the bromide containing clusters. This observation is characteristic of the weaker bromide–H_2S interaction.

The stretching modes are the most informative of the effects of cluster H-bonding, and we will restrict our discussion to these from this point forward.

For both clusters, two strong S–H stretching bands are predicted, corresponding to the concerted antisymmetric and symmetric stretching motion of the hydrogens in contact with the anion. In these clusters, the symmetric stretch lies to higher wavenumber. The H-bonded S–H stretches for both clusters have shifted to higher wavenumber when compared with the dimer complexes, indicating a reduction in the strength of the halide–H_2S interaction. This also evident from a smaller binding energy of the dimer and trimer clusters, for example in the case of chloride the binding energy reduces from −13.6 to −10.5 kcal mol^{-1}.

Weaker bands are predicted to higher wavenumber from the H-bonded S–H stretches, and correspond to motion of the hydrogens not involved with the anion–H_2S H-bonding. The stronger of these two modes is shown in the inset of Fig. 7, and corresponds to the H-bonded hydrogen of the $HSH\cdots SH_2$ bond.

The predicted binding energies of the chloride and bromide–$(H_2S)_2$ trimer clusters, 3672 and 3288 cm^{-1}, indicate that vibrational predissociation is not a feasible method to study these clusters. Again, using argon tagging should help resolve this problem, and allow one to investigate the S–H stretch region experimentally.

C. Tetramer clusters: Cl^-–$(H_2S)_3$ and Br^-–$(H_2S)_3$

I. Structures and energetics. The chloride–$(H_2S)_3$ tetramer clusters were investigated at the MP2/aug-cc-pvdz and -pvtz levels. The bromide–$(H_2S)_3$ clusters were investigated at the MP2/aug-cc-pvdz as using the larger basis set requires more

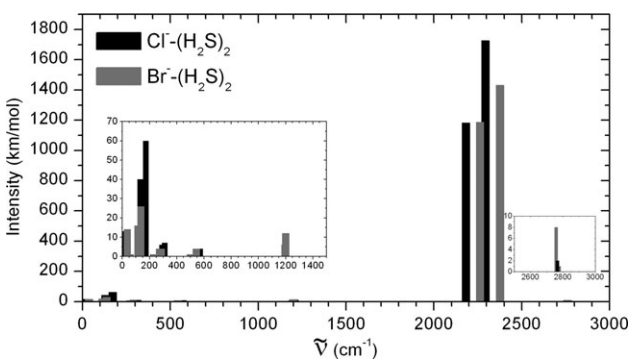

Fig. 7 Predicted IR spectra of the Cl^-–$(H_2S)_2$ and Br^-–$(H_2S)_2$ trimer clusters at the MP2/aug-cc-pvtz level.

computational effort than is justified, especially as comparisons between results for the two different basis sets for the bromide clusters showed that the smaller aug-cc-pvdz set produces sufficiently accurate results.

For both chloride and bromide cluster series, we found three minima and three higher order stationary points, as shown in Fig. 8. The three minima are of C_3, C_s, and C_1 symmetry and all involve HSH$\cdots$SH$_2$ H-bonding, confirmed by NBO analyses. For the C_3 isomer, each H_2S molecule donates and accepts a solvent–solvent H-bond. The solvent molecules of the C_1 isomer form a chain motif, with only the middle H_2S accepting and donating a H-bond. And, lastly the C_s isomer features one H_2S receiving H-bonds from two others. As shown in the following discussion of the cluster vibrational properties, the structural differences between the clusters lead to quite different predicted spectra which can help in identifying which isomer is present in experimental studies.

For both the chloride and bromide tetramer clusters, the three minima are predicted to lie very close in energy (after zpe and BSSE corrections are made to the electronic energies), so it is impossible to state conclusively which of the three is the global minimum. The ordering of the isomers is the same for chloride and bromide clusters. We calculated the enthalpy of ligand association of the C_3 symmetry clusters, and found values of -10.0 and -8.6 kcal mol^{-1} for the chloride and bromide clusters, respectively.

When we compare the predicted structures of this cluster size with the corresponding fluoride clusters,[11] we see that there are now common structures, the C_3 and C_s symmetry isomers. In fact, for the corresponding fluoride clusters, this was the first cluster size for which a 'solvated anion' structure was observed. In the present study, due to the larger proton affinity of SH^- compared with both Cl^- and Br^- we only observe 'solvated anion' structural motifs.

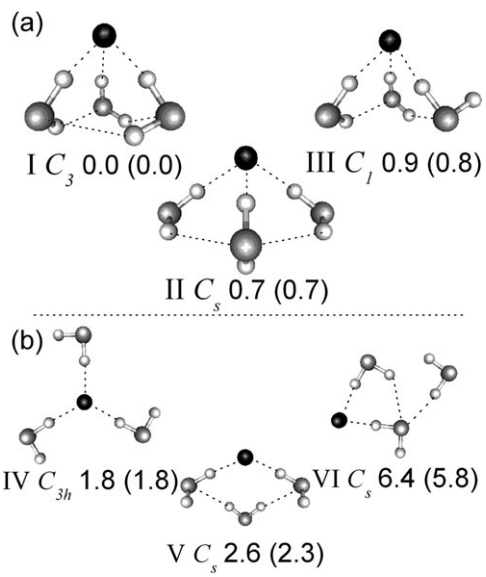

Fig. 8 Predicted structures of the Cl^-–$(H_2S)_3$ tetramer clusters. Similar structures are predicted for the bromide tetramer clusters. (a) corresponds to minima, while (b) are higher order stationary points (IV with six imaginary frequencies, V with one, and VI with two). Numbers correspond to BSSE and zpe corrected energy differences compared with the global minimum, bromide values are in parentheses.

II. Predicted infrared spectra. The predicted IR spectra of the three minima of the tetramer clusters are provided in Fig. 9, and a complete list of frequencies are given in the ESI.† Here we discuss only the S–H stretching bands, as these display the greatest effects of cluster formation with the halide anion. The bands are labelled in the figure in the following way; $\omega_{bi}^{a/s}$ corresponds to a concerted antisymmetric or symmetric stretching mode of the S–H groups H-bonded to the ion, and $\omega_{bs}^{a/s}$ a vibration of an S–H group H-bonded to another H_2S. The bands of the bromide clusters are not labelled, however due to the similarity in the form of the spectra it is possible to identify the corresponding bands.

On first inspection, the differences between the spectra of the three minima are obvious. For example, in the case of the C_3 isomer there are only two strong S–H stretching bands, whereas for the other isomers of lower symmetry there are three. This alone would aid in proving, or disproving, the existence of the C_3 isomer. With regard to the other two isomers, there are marked differences in the band spacings and intensities to aid in discriminating between the two, should experimental spectra be recorded.

One notices that the H-bonded stretching bands of the bromide clusters are shifted to higher wavenumber compared with the chloride clusters due to the weaker Br^-–H_2S interactions. We find however that the stretches of the free S–H groups (those not involved in cluster bonding) are shifted to lower wavenumber, indicative of a weaker bond. We believe however that this is due to using the MP2/aug-cc-pvdz level for bromide, as this led to slightly larger terminal S–H bond lengths, and hence red shifted stretching bands (see ESI for the Br^-–$(H_2S)_2$ trimer cluster).

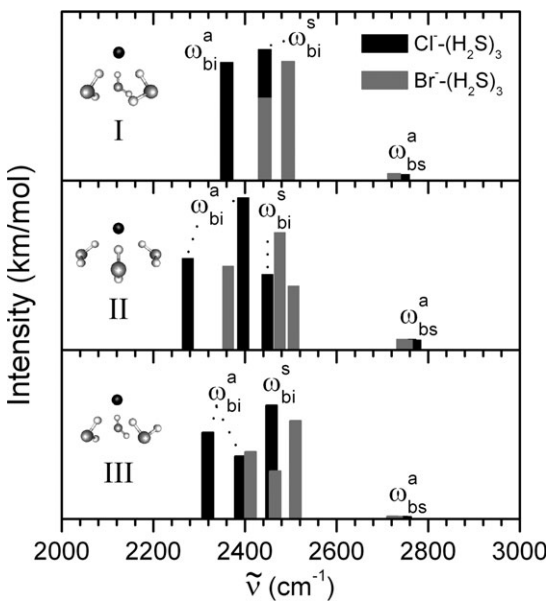

Fig. 9 Predicted infrared spectra of the Cl^- and Br^-–$(H_2S)_3$ clusters over the S–H stretch region. Full lists of vibrational frequencies are given in the ESI.†

D. Pentamer clusters: Cl^-–$(H_2S)_4$ and Br^-–$(H_2S)_4$

I. Structures and energetics. The pentamer X^-–$(H_2S)_4$ was the largest cluster size investigated in the current study, at the MP2/aug-cc-pvdz level of theory. For both the chloride and bromide clusters, we found six stationary points, shown in Fig. 10. Of these stationary points, four are minima and the remaining two are higher order points.

Aside from the C_{4h} higher order stationary point, all of the cluster forms display H-bonds between the H_2S molecules and the anion, and also $HSH\cdots SH_2$ H-bonding. These interactions are confirmed to be H-bonding through NBO analyses which predict electron density transfer from the H-bond acceptor to the σ* anti-bonding orbital of the H-bond donator.

For both the chloride and bromide pentamer clusters, the four minima are predicted to lie very close in energy, with the largest separation being between isomers I and IV (after zpe and BSSE corrections are made to the electronic energies). Therefore, as with the tetramer clusters it is not possible to state conclusively which of the four is the global minimum on the potential energy surface. The ordering of the isomers is the same for chloride and bromide clusters. We calculated the enthalpy of ligand association of the C_1 symmetry clusters (labelled I in Fig. 10), and found values of −7.4 and −6.8 kcal mol^{-1} for the chloride and bromide clusters, respectively. These were calculated with respect to MP2/aug-cc-pvdz results of the $n = 3$ tetramer clusters. The enthalpies of the ligand association reactions for all of the clusters investigated in this study are summarised in Table 1. The decrease in the enthalpy of ligand association, or ligand binding energy, can be clearly seen. The differences in binding energies between the two levels of theory is within chemical accuracy (1 kcal mol^{-1}).

Table 1 Predicted enthalpies for ligand association reactions at 298 K, $\Delta H_{n-1\rightarrow n}^{298\ K}$, in kcal mol^{-1} at the MP2/aug-cc-pvtz level. Numbers in parentheses are differences between MP2/aug-cc-pvtz and MP2/aug-cc-pvdz values

n	Cl^-–$(H_2S)_n$/kcal mol^{-1}	Br^-–$(H_2S)_n$/kcal mol^{-1}
1	−13.6 (−0.9)	−11.1 (−0.8)
2	−10.5 (−0.9)	−9.4 (−0.7)
3	−10.0 (−0.8)	−8.6[a]
4	−7.4[a]	−6.8[a]

[a] Calculated at MP2/aug-cc-pvdz level.

II. Predicted infrared spectra. Predicted infrared spectra for the four minima are provided in Fig. 11. For clarity, only the chloride spectra are shown, as the bromide spectra are similar only shifted to higher wavenumber. Again, we restrict our discussion to the S–H stretching bands which lie around 2500 cm^{-1}, as these vibrations exhibit the greatest effect from H-bonding of the ligands to the anion. In the figure, the band associated with symmetric stretching of the S–H groups H-bonded to the anion is labelled $\omega_{bi}^{a/s}$. The other strong bands are associated with antisymmetric type stretches. The weak bands at around 2780 cm^{-1} are due to vibrations associated with the non-bonded S–H groups, or SH groups involved in $HSH\cdots SH_2$ H-bonding.

One can see instantly that there are differences in the predicted spectra of the four minima in the region of the H-bonded S–H stretching modes (H-bonded to the anion). For example, the spectrum of isomer II shows only two strong bands, due to the C_4 symmetry of the isomer. For isomer I, the H-bonded S–H stretching modes are grouped together in one compact region, indicative of roughly equivalent H_2S units. In essence, the pattern of the bands is different for each isomer,

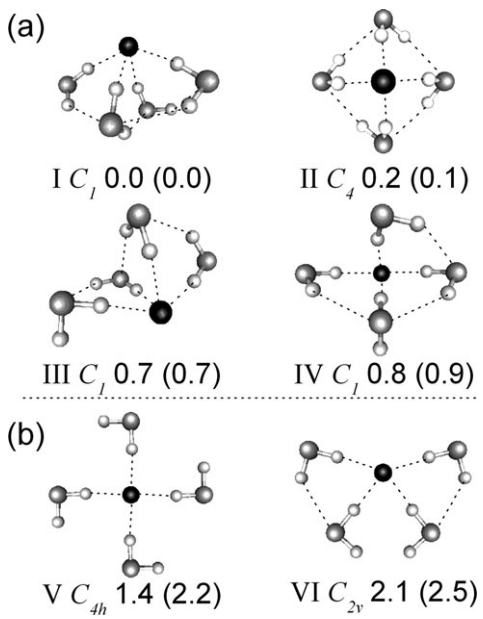

Fig. 10 Predicted structures of the Cl^- and Br^-–$(H_2S)_4$ pentamer clusters at the MP2/aug-cc-pvdz level, with (a) being minima, and (b) higher order stationary points (V and VI with eight and three imaginary frequencies, respectively). Numbers correspond to zpe and BSSE corrected energy differences, bromide values are in parentheses.

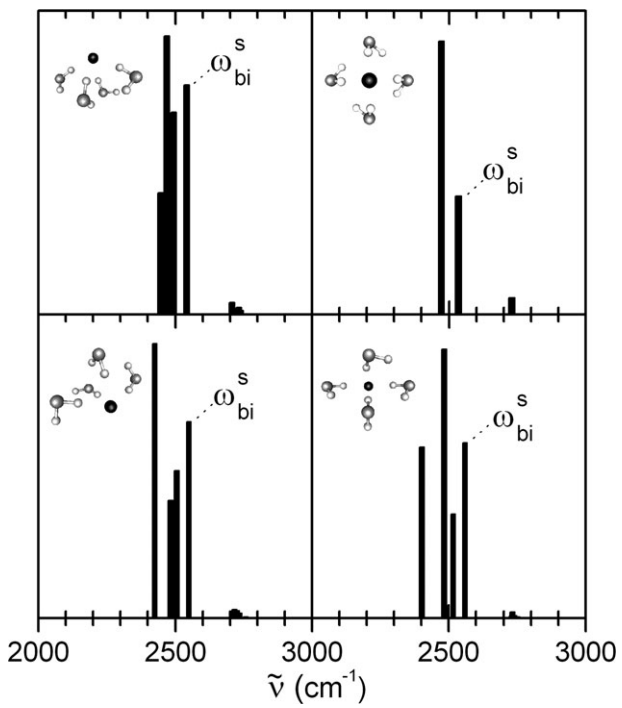

Fig. 11 Predicted IR spectra of the Cl^-–$(H_2S)_4$ pentamer clusters at the MP2/aug-cc-pvdz level.

and therefore we believe that these predications, in combination with experimental spectra, should permit identification of the dominant form of the cluster.

Comparing the predicted spectra of the tetramer and pentamer clusters, one observes that the bands have shifted slightly to higher wavenumber (comparing MP2/aug-cc-pvdz results). This is again an indication that the H-bond strength between any one ligand and the anion core has decreased. This is supported by the decrease in the enthalpy of ligand association, decreasing for example from −9.2 to −7.4 kcal mol^{-1} for the chloride clusters (again MP2/aug-cc-pvdz results, calculated for the lowest energy isomer).

Finally, for the chloride clusters the predicted ligand binding energy (around 2590 cm^{-1}) is larger than the energy of vibrational modes associated with motion of the hydrogens H-bonded to the anions. Therefore, dissociation of the Cl^-–$(H_2S)_4$ clusters from absorption of a single photon is not energetically possible. As discussed for the smaller clusters, the use of argon tagging of the cluster will allow them to be probed experimentally. The situation is different for the bromide pentamer clusters however, as the ligand binding energy is predicted to be around 2380 cm^{-1}. For these clusters it should be possible to record one photon spectra of the bare clusters (refer to the ESI† for Br^-–$(H_2S)_4$ vibrational frequencies).

3. Conclusions

The findings of this study can be summarised as follows;

(1) Clusters formed from neutral H_2S ligands and the chloride and bromide anions display "solvated anion" structural forms where the neutral H_2S ligands bind to the anion *via* H-bonds. The structural motif is a consequence of the larger proton affinity of the SH^- anion compared with Cl^- and Br^-.

(2) The binding energy of the Cl^-–H_2S and Br^-–H_2S dimer complexes are predicted to be −13.6 and −11.1 kcal mol^{-1}, respectively. The binding energies of subsequent ligands decrease.

(3) Vibrational frequencies, corrected for anharmonicity, were produced for the dimer complexes using two methods, CC-VSCF and simple one dimensional potential energy curves. The H-bonded S–H stretching modes were predicted to occur at 1389 and 1893 cm^{-1} for the chloride and bromide–H_2S complexes, respectively.

(4) The infrared bands associated with motion of the H-bonded S–H groups shifted to higher wavenumber on increased cluster size. The shifts are in line with the decreased anion–ligand binding energies.

It will be interesting to see if the results presented in this article are supported by experiments on isolated gas phase halide–H_2S clusters Or, indeed if vibrational analyses derived from multidimensional potential energy surfaces are in support of our predictions based on the VSCF procedure.

Acknowledgements

We thank Martin Fechner (MPI) for assistance with work stations, the MPI für biophysikalische Chemie and the Alexander von Humboldt foundation for financial support.

References

1 D. M. Neumark, *J. Chem. Phys.*, 2006, **125**, 132–303.
2 D. M. Neumark, *Phys. Chem. Chem. Phys.*, 2005, **7**, 433.
3 W. H. Robertson and M. A. Johnson, *Annu. Rev. Phys. Chem.*, 2003, **54**, 173.
4 Z. M. Loh, R. L. Wilson, D. A. Wild, E. J. Bieske, J. M. Lisy, B. Njegic and M. S. Gordon, *J. Phys. Chem. A*, 2006, **110**, 13736.
5 Z. M. Loh, R. L. Wilson, D. A. Wild, E. J. Bieske and M. S. Gordon, *Aust. J. Chem.*, 2004, **57**, 1157.
6 P. Weis, P. R. Kemper, M. T. Bowers and S. S. Xantheas, *J. Am. Chem. Soc.*, 1999, **121**, 3531.
7 O. M. Cabarcos, C. J. Weinheimer, J. M. Lisy and S. S. Xantheas, *J. Chem. Phys.*, 1999, **110**, 5.
8 M. Masamura, *J. Chem. Phys.*, 2003, **118**, 6336.
9 M. Masamura, *J. Chem. Phys.*, 2002, **117**, 5257.
10 D. A. Wild and T. Lenzer, *Phys. Chem. Chem. Phys.*, 2004, **6**, 5122.
11 D. A. Wild and T. Lenzer, *Phys. Chem. Chem. Phys.*, 2005, **7**, 3793.
12 K. Rempala and K. M. Ervin, *J. Chem. Phys.*, 2000, **112**, 4579.
13 J. D. D. Martin and J. W. Hepburn, *J. Chem. Phys.*, 1998, **109**, 8139.
14 C. Blondel, P. Cacciani, C. Delsart and R. Trainham, *Phys. Rev. A*, 1989, **40**, 3698.
15 M. Masamura, *Int. J. Quantum Chem.*, 2004, **100**, 28.
16 J. E. Del Bene, *Struct. Chem.*, 1989, **1**, 19.
17 J. W. Larson and T. B. McMahon, *J. Am. Chem. Soc.*, 1987, **109**, 6230.
18 H. E. Dorsett, R. O. Watts and S. S. Xantheas, *J. Phys. Chem. A*, 1999, **103**, 3351.
19 P. Ayotte, S. B. Nielsen, G. H. Weddle, M. A. Johnson and S. S. Xantheas, *J. Phys. Chem. A*, 1999, **103**, 10665.
20 S. S. Xantheas, G. S. Fanourgakis, S. C. Farantos and M. Velegrakis, *J. Chem. Phys.*, 1998, **108**, 46.
21 R. A. Kendall, T. H. Dunning and R. J. Harrison, *J. Chem. Phys.*, 1992, **96**, 6796.
22 D. E. Woon and T. H. Dunning, *J. Chem. Phys.*, 1993, **98**, 1358.
23 T. H. Dunning, *J. Chem. Phys.*, 1989, **90**, 1007.
24 S. F. Boys and F. Bernardi, *Mol. Phys.*, 1970, **19**, 553.
25 G. M. Chaban, J. O. Jung and R. B. Gerber, *J. Chem. Phys.*, 1999, **111**, 1823.
26 M. W. Schmidt, K. K. Baldridge, J. A. Boatz, S. T. Elbert, M. S. Gordan, J. H. Hensen, S. Koseki, N. Matsunaga, K. A. Nguyen, S. J. Su, T. L. Windus, M. Dupuis and J. A. Montgomery, *J. Comput. Chem.*, 1993, **14**, 1347.
27 A. E. Reed, L. A. Curtiss and F. Weinhold, *Chem. Rev.*, 1988, **88**, 899.
28 J. E. Del Bene, H. D. Mettee, M. J. Frisch, B. T. Luke and J. A. Pople, *J. Phys. Chem.*, 1983, **87**, 3279.
29 M. J. Frisch, G. W. Trucks, H. B. Schlegel, G. E. Scuseria, M. A. Robb, J. R. Cheeseman, J. A. Montgomery, Jr., T. Vreven, K. N. Kudin, J. C. Burant, J. M. Millam, S. S. Iyengar, J. Tomasi, V. Barone, B. Mennucci, M. Cossi, G. Scalmani, N. Rega, G. A. Petersson, H. Nakatsuji, M. Hada, M. Ehara, K. Toyota, R. Fukuda, J. Hasegawa, M. Ishida, T. Nakajima, Y. Honda, O. Kitao, H. Nakai, M. Klene, X. Li, J. E. Knox, H. P. Hratchian, J. B. Cross, V. Bakken, C. Adamo, J. Jaramillo, R. Gomperts, R. E. Stratmann, O. Yazyev, A. J. Austin, R. Cammi, C. Pomelli, J. Ochterski, P. Y. Ayala, K. Morokuma, G. A. Voth, P. Salvador, J. J. Dannenberg, V. G. Zakrzewski, S. Dapprich, A. D. Daniels, M. C. Strain, O. Farkas, D. K. Malick, A. D. Rabuck, K. Raghavachari, J. B. Foresman, J. V. Ortiz, Q. Cui, A. G. Baboul, S. Clifford, J. Cioslowski, B. B. Stefanov, G. Liu, A. Liashenko, P. Piskorz, I. Komaromi, R. L. Martin, D. J. Fox, T. Keith, M. A. Al-Laham, C. Y. Peng, A. Nanayakkara, M. Challacombe, P. M. W. Gill, B. G. Johnson, W. Chen, M. W. Wong, C. Gonzalez and J. A. Pople, *GAUSSIAN 03 (Revision B.04)*, Gaussian, Inc., Pittsburgh, PA, 2003.
30 L. Laaksonen, *J. Mol. Graphics*, 1992, **10**, 33.
31 D. L. Bergman and L. Laaksonen, *J. Mol. Graphics*, 1997, **15**, 301.
32 G. M. Chaban, S. S. Xantheas and R. B. Gerber, *J. Phys. Chem. A*, 2003, **107**, 4952.
33 K. Yagi, K. Hirao, T. Taketsugu, M. W. Schmidt and M. S. Gordon, *J. Chem. Phys.*, 2004, **121**, 1383.
34 R. J. Le Roy. University of Waterloo, *Chem. Phys. Research*, Report No. CP-655, 2002.

35 D. A. Wild, Z. M. Loh, R. L. Wilson and E. J. Bieske, *Chem. Phys. Lett*., 2003, **369**, 684.
36 J. M. Weber, J. A. Kelley, S. B. Nielsen, P. Ayotte and M. A. Johnson, *Science*, 2000, **287**, 2461.
37 P. Ayotte, G. H. Weddle, J. Kim and M. A. Johnson, *Chem. Phys*., 1998, **239**, 485.
38 P. Ayotte, J. A. Kelley, S. B. Nielsen and M. A. Johnson, *Chem. Phys. Lett*., 2000, **316**, 455.
39 Y. X. Zhao, I. Yourshaw, G. Reiser, C. C. Arnold and D. M. Neumark, *J. Chem. Phys*., 1994, **101**.
40 T. Lenzer, I. Yourshaw, M. R. Furlanetto, G. Reiser and D. M. Neumark, *J. Chem. Phys*., 1999, **110**, 9578.

